THE JOURNAL OF BIOLOGICAL CHEMISTRY VOL. 286, NO. 18, pp. 16285–16296, May 6, 2011
© 2011 by The American Society for Biochemistry and Molecular Biology, Inc. Printed in the U.S.A.

A Phosphodiesterase 3B-based Signaling Complex Integrates Exchange Protein Activated by cAMP 1 and Phosphatidylinositol 3-Kinase Signals in Human Arterial Endothelial Cells*[S]

Received for publication, December 28, 2010, and in revised form, March 8, 2011 Published, JBC Papers in Press, March 10, 2011, DOI 10.1074/jbc.M110.217026

Lindsay S. Wilson[‡1], George S. Baillie[§], Lisa M. Pritchard[‡], Bibiana Umana[¶], Anna Terrin[§], Manuela Zaccolo[§], Miles D. Houslay[§], and Donald H. Maurice[‡¶2]

From the Departments of [‡]Pathology and Molecular Medicine and [¶]Pharmacology and Toxicology, Queen's University, Kingston, Ontario K7L 3N6, Canada and the [§]Molecular Pharmacology Group, Institute of Biomedical and Life Sciences, University of Glasgow, Glasgow, G12 8QQ, United Kingdom

Enzymes of the phosphodiesterase 3 (PDE3) and PDE4 families each regulate the activities of both protein kinases A (PKAs) and exchange proteins activated by cAMP (EPACs) in cells of the cardiovascular system. At present, the mechanisms that allow selected PDEs to individually regulate the activities of these two effectors are ill understood. The objective of this study was to determine how a specific PDE3 variant, namely PDE3B, interacts with and regulates EPAC1-based signaling in human arterial endothelial cells (HAECs). Using several biochemical approaches, we show that PDE3B and EPAC1 bind directly through protein-protein interactions. By knocking down PDE3B expression or by antagonizing EPAC1 binding with PDE3B, we show that PDE3B regulates cAMP binding by its tethered EPAC1. Interestingly, we also show that PDE3B binds directly to p84, a PI3Kγ regulatory subunit, and that this interaction allows PI3Kγ recruitment to the PDE3B-EPAC1 complex. Of potential cardiovascular importance, we demonstrate that PDE3B-tethered EPAC1 regulates HAEC PI3Kγ activity and that this allows dynamic cAMP-dependent regulation of HAEC adhesion, spreading, and tubule formation. We identify and molecularly characterize a PDE3B-based "signalosome" that integrates cAMP- and PI3Kγ-encoded signals and show how this signal integration regulates HAEC functions of importance in angiogenesis.

The ubiquitous intracellular messenger cAMP regulates human arterial endothelial cell (HAEC)[3] adhesion, migration, and permeability (1–3) by activating two groups of effectors, the protein kinases A (PKAs) and the exchange proteins activated by cAMP (EPACs). Specificity in cAMP signaling through these effectors is mediated by their selective subcellular localization via interactions with anchoring or tethering proteins (4, 5). In addition, selective signaling by these anchored/tethered complexes is critically dependent on integration of cyclic nucleotide phosphodiesterases (PDEs) (2, 4, 6), because these enzymes regulate local effector activities through targeted cAMP hydrolysis. HAECs express variants from several of the 11 families of PDEs (7) with potential for the generation of multiple, distinct PKA-based, or EPAC-based signaling complexes (2). Currently, little is known concerning the identities of the individual PDEs that coordinate localized activation of PKAs or EPACs, in HAECs and the downstream signaling events altered by activation of individual HAEC cAMP signaling complexes (8).

Global activation of EPAC promotes accumulation of GTP-bound and activated Rap and/or R-Ras. Activated Rap or R-Ras can signal via activation of several effectors, including phospholipase Cϵ, phospholipase D, Raf-1, p38 MAPK, and PI3K (9–11). Four distinct class 1 PI3K enzymes (class 1A (PI3Kα, β, δ) and class 1B (PI3Kγ)) control numerous cellular processes (12–14). Class-specific PI3K catalytic subunits (p110α, β, δ, and γ) gain access to their membrane phosphatidylinositol substrates through binding regulatory subunits. In the case of PI3Kγ, p110γ selectively interact with one of two regulatory subunits (p101 or p84), both of which associate with membranes by binding heterotrimeric G protein-derived βγ-subunit dimers (15–18). PI3Kγ is also activated by Ras-dependent mechanisms (19, 20).

Integration of cAMP-EPAC1 and PI3Kγ-encoded signals is known to occur in cells (21, 22). Herein we report that a cyclic nucleotide phosphodiesterase (PDE3B) assembles a HAEC signalosome that contains both EPAC1 and the p84-regulated form of PI3Kγ (p84-p110γ). In addition, we show that this signalosome allows integration of cAMP-EPAC1- and PI3Kγ-encoded signals and that this integration controls several HAEC functions of importance to angiogenesis.

* This work was supported by Canadian Institutes of Health Research Grant MOP57699 (to D. H. M.), Medical Research Council Grant G0600765 (to M. D. H. and G. S. B.), and Fondation Leducq Grant 06CVD02.

[S] The on-line version of this article (available at http://www.jbc.org) contains supplemental Figs. S1–S3.

[1] Recipient of a Canadian Institutes of Health Research Doctoral Research Award.

[2] Career Investigator of the Heart and Stroke Foundation of Ontario through Grant CI 5962. To whom correspondence should be addressed: Dept. of Pharmacology & Toxicology, Botterell Hall, A208, Queen's University, Kingston, ON K7L 3N6, Canada. Fax: 613-533-6412; E-mail: mauriced@queensu.ca.

[3] The abbreviations used are: HAEC, human arterial endothelial cells; 8-pCPT-2′-O-Me-cAMP, 8-(4-chlorophenylthio)adenosine-3′,5′-cAMP; EPAC, exchange protein activated by cAMP; EPAC1-DP, EPAC1 displacing peptide; EPAC1-NDP, EPAC1 nondisplacing peptide; PDE, cyclic nucleotide phosphodiesterase.

EXPERIMENTAL PROCEDURES

Materials—The FLAG-tagged p84 and p101 regulatory domains were provided by Michael Schaefer (Berlin, Germany). p110γ-cDNA construct was provided by Emilio Hirsch (Torino, Italy). CFP-YFP-tagged EPAC1 constructs were a generous gift from Manuela Zaccolo (Glasgow, UK), and the FLAG-EPAC1 was a gift from Xiaodong Cheng (Galveston, TX). ERK, PKB, and EPAC1 antibodies were from Cell Signaling. M2-FLAG antibody was from Sigma-Aldrich, whereas R-Ras and Rap1 antibodies were from Santa Cruz. The GFP antibody was purchased from Invitrogen, whereas the PDE3B antibody was a gift from ICOS Corp., and the PI3Kγ antibody was a gift from Emilio Hirsch (Torino, Italy). The p84 antibody was a gift from Len Stephens (Cambridge, UK), and the p101 antibody was from Abcam. The PI3Kγ-specific inhibitor (AS-604850) was a gift from Phillip Thompson (Melbourne, Australia), and 8-pCPT-2′-O-Me-cAMP was from Biolog Life Sciences.

Cell Culture and Transfection—HAECs (Lonza) were cultured in EGM-2 medium as described previously (3) and when appropriate transfected with siRNAs targeted to PDE3B, EPAC1, p84, p101, or a control siRNA (Invitrogen) at 300 pmol/100-mm dish with Lipofectamine 2000. 293T cells were cultured and transfected as previously described (4).

RNA Interference—The PDE3B siRNA was HSS107710: 5′-GCCUCACCAAGAAUUUGGCAUUUCA-3′ (sense) with 5′-CGGAGUGGUUCUUAAACCGAAAGU-3′ (antisense). The EPAC1 siRNA was HSS115938: 5′-AUUGAGAUUCUUCUGCUCCUUGAGG-3′ (sense) with 5′-UAACUCUAAGAAGACGAGGAACUCC-3′. The p84 siRNA was HSS152254: 5′-CCGCCAUCCACAUGGCUGAGAU-3′ (sense) with 5′-GGCGGUAGGUGUUCGACCGACUCUA-3′ (antisense). The p101 siRNA was HSS118911: 5′-ACUCCAAAUCCAAGAAGGGCUUUAA-3′ (sense) with 5′-UUAAAGCCCUUCUUGGAUUUGGAGU-3′ (antisense). The Rap1 siRNA was HSS109049: 5′-ACGACUUACCGGACCUGAGGGAACA-3′ (sense) with 5′-UGUUCCCUCAGGUCCUGUAAGUCGU-3′ (antisense). The R-Ras siRNA was HSS184464: 5′-GGGCUGUCCGGAAAUACCAGGAACA-3′ (sense) with 5′-UGUUCCUGGUAUUUCCGGACAGCCC-3′ (antisense).

RT-PCR Amplification of mRNA Encoding HAEC p84 and p101—Total RNA was extracted using the Qiagen RNeasy purification kit, and 200 ng of total RNA was used as the template for synthesis of cDNA with a Qiagen one-step RT-PCR kit. p84 and p101 levels were amplified using gene-specific primers targeted to p84 (5′-CGAGCCGGGAGGGACACGTA-3′ (sense) and 5′-GAAACCCGGGCCAACTCCCG-3′ (antisense)) and p101 (5′-GGGTCACTCCGCTGCCACAC-3′ (sense) and 5′-GCGTCAGGGCCTCCATGCTG-3′ (antisense). The reaction mixture was amplified for 35 cycles.

Protein-Protein Interaction Studies—The cell lysates for immunoprecipitations were generated as previously described (3). Briefly, detergent-supplemented lysates were precleared with protein A/G-agarose and 1 μg of mouse IgG (3 h at 4 °C). Precleared lysates were then incubated (16 h at 4 °C) with either cAMP-conjugated agarose (Sigma; for cAMP-agarose pulldowns) or M2-FLAG agarose (Sigma; FLAG immunoprecipitations) or mouse IgG (Santa Cruz) or PDE3B antisera (ICOS Corp; for PDE3B pulldowns). Proteins in isolated complexes were detected by SDS-PAGE and immunoblot analysis. Subcellular fractions were prepared by centrifugation, and membrane-containing fractions were resuspended in detergent-supplemented buffer (0.1% SDS, 0.5% sodium deoxycholate, and 1% Igepal).

Cell Signaling Studies—HAECs were transfected with indicated siRNA as described. The cells were serum-starved overnight and treated with 10 μmol/liter EPAC1-NDP or EPAC1-DP for 4 h when indicated. The cells were treated with indicated test reagents and lysed by homogenization using a Tenbroeck tissue grinder in a Tris (50 mM, pH 7.4)-based lysis buffer supplemented with 1% Triton-X-100, 150 mM sodium chloride, 10 mM sodium pyrophosphate, 10 mM sodium β-glycerophosphate, 10 mM sodium fluoride, 1 μg/ml pepstatin A, 1 μg/ml E-64, 20 μg/ml bestatin, 100 μg/ml PMSF, 1 μg/ml aprotinin, 1 μg/ml leupeptin, 5 mM benzamidine, 10 mM sodium orthovanadate on ice. When membrane fractions were analyzed, the cells were lysed in detergent-free lysis buffer as described above and centrifuged to isolate membrane fractions that were resuspended in detergent supplemented lysis buffer. The cell lysates were analyzed by SDS-PAGE and immunoblotting.

Rap and Ras Activation Assay—HAECs were serum-starved for 24 h in 0.1% FBS-containing medium. The cells were treated with 100 μmol/liter 8-pCPT-2′-O-Me-cAMP for 5 min and lysed in Mg^{2+}-containing lysis buffer (25 mmol/liter HEPES, pH 7.5, 150 mmol/liter NaCl, 1% Igepal CA-630, 0.25% sodium deoxycholate, 10% glycerol, 25 mmol/liter NaF, 10 mmol/liter $MgCl_2$, 1 mmol/liter EDTA, 1 mmol/liter sodium orthovanadate, 10 μg/ml leupeptin, 10 μg/ml aprotinin). The cell lysates were incubated with either Ral-GDS or Raf-RBD-agarose (Millipore) for 30 min at 4 °C. Isolated proteins were analyzed by SDS-PAGE.

Adhesion Assay—Adhesion assays were performed as previously described (3). HAECs were incubated with adenine (4 μmol/liter, 2 μCi of [^{3}H]adenine/ml) for 16 h. The cells were rinsed free of unincorporated [^{3}H]adenine and incubated with EPAC1-NDP, EPAC1-DP, or no peptide for 4 h. The cells were trypsinized, and labeled cells (20 000) were allowed to adhere to fibronectin-coated wells in the presence or absence of test reagents. The cells were rinsed and dissolved in 0.1% Triton X-100, transferred to scintillation vials, and counted by liquid scintillation. The values are expressed as the means ± S.E. For immunostaining, HAECs were allowed to adhere to fibronectin-coated coverslips for 15 min, fixed, and stained for PDE3B and EPAC1.

Fluorescence Resonance Energy Transfer Imaging—FRET imaging experiments were performed as previously described (27). Briefly, FRET experiments were performed 24–48 h after HEK 293 cell transfection. The cells were maintained at room temperature and imaged on an inverted microscope (Olympus IX50). The images were acquired using custom-made software, and FRET changes were measured as changes in the background-subtracted 480/545 nm fluorescence emission intensity on excitation at 430 nm and expressed as R/R_o, where R is

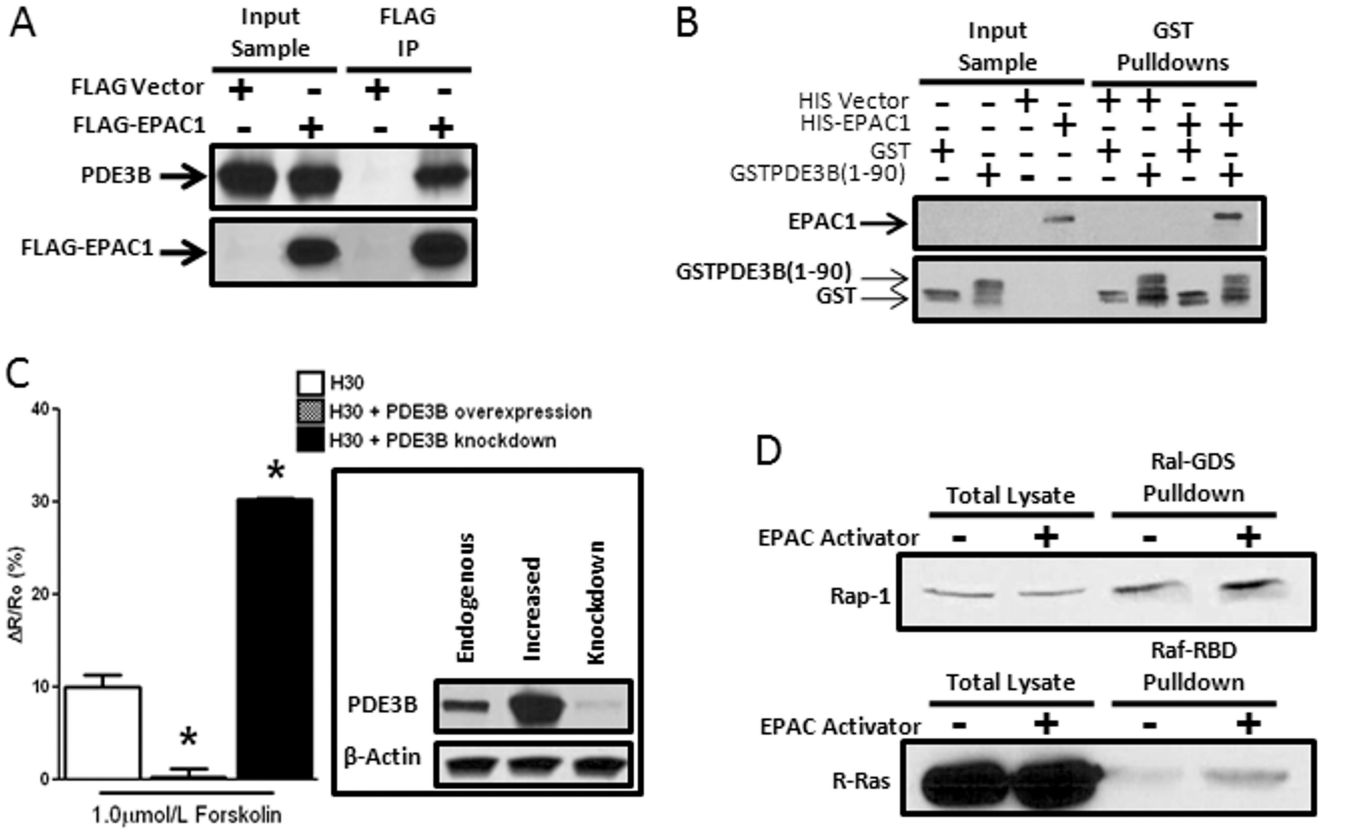

FIGURE 1. **PDE3B tethers and regulates EPAC1.** *A*, 293T cells lysates expressing either FLAG or FLAG-tagged EPAC1 were subjected to anti-FLAG immunoprecipitations (*IP*, M2-agarose, 4 °C, 16 h). Immune complexes were resolved by SDS-PAGE and immunoblotted for PDE3B or FLAG. A representative immunoblot is shown, and similar results were obtained in at least 10 separate experiments. *B*, bacterially expressed/purified His_6-tagged EPAC1 that bound either GST- or GST-PDE3B[1–90]-saturated GSH-Sepharose beads was isolated and detected by immunoblot analysis. A representative immunoblot from three similar experiments is shown. *C*, EPAC1-based cAMP sensor (H30) binding of cAMP in response to forskolin in cells expressing increased PDE3B or after PDE3B knockdown was measured by FRET. The values are the means ± S.E. from multiple measures in four separate experiments. *, significant differences ($p < 0.05$) between control and each condition. *D*, accumulation of GTP-bound Rap-1 or R-Ras following 8-pCPT-2′-O-Me-cAMP (0.1 mmol/liter, 5 min) incubation were measured by adsorption with RalGDS- or RafRBD-agarose, respectively, and immunoblotting. A representative immunoblot from three similar experiments is shown.

the ratio at time t, and R_o is the ratio at time $t = 0$ s. The values are expressed as the means ± S.E.

SPOT Synthesis of Peptides and Overlay Experiments—Overlapping sequences of either EPAC1 or PDE3B were synthesized on continuous cellulose membrane supports by the AutoSpot-Robot ASS 222 (Intavis Bioanalytical Instruments). The interaction of spotted peptides with FLAG-tagged fusion proteins was determined by overlaying the cellulose membranes with cell lysates expressing either FLAG-EPAC, FLAG-PDE3B, FLAG-p84, or control lysate, and detection was performed using anti-mouse antibodies coupled with HRP.

Tube Formation Assays and Measurement of Cell Area—Growth factor-reduced Matrigel (BD Biosciences) (50 μl/2.0 cm) was gelled (37 °C, 1 h). Following labeling of HAEC (0.5 μmol/liter Cell-Tracker (Invitrogen), 30 min), 125,000 cells were plated in EGM-2 medium in the presence or absence of indicated agents. Live cell tube formation was observed using fluorescence, and the images were acquired using a Zeiss Axiovert S100 microscope equipped with a Plan-Neofluor 5× objective and a Cooke SensiCam at fixed intervals over a 16-h period. For fixed cell staining, the cells were processed as described (3). The mean cell area was measured (number of pixels occupied), and the values were calculated using Image J.

Statistical Analysis—The values are presented as the means ± S.E. from at least three independent experiments. HAEC adhesion assays and tube formation assays were performed in quadruplicate determinations within experiments, and each condition was measured in multiple experiments. Effects of test reagents on phosphorylation status, binding competition, adhesion, PDE activity, FRET measurements, and tube formation were tested for significance using a Neuman post hoc test, with $p < 0.05$ considered significant. When representative immunoblots or immunostains were shown, similar data were obtained at least four times.

RESULTS

PDE3B Directly Binds and Regulates EPAC1—Immunoprecipitation of expressed FLAG-tagged EPAC1 allows recovery of endogenous 293T PDE3B (Fig. 1*A*), indicating that these proteins interact in cells. Also, bacterially expressed/purified His-tagged EPAC1 interacts selectively with a bacterially expressed/purified GST fusion encoding residues 1–90 of PDE3B (Fig. 1*B*), demonstrating that these proteins interact directly with each other in solution. EPAC1 binding of cAMP was reduced in HEK293 cells overexpressing PDE3B and increased in cells with reduced PDE3B (Fig. 1*C*), indicating that PDE3B catalytic activ-

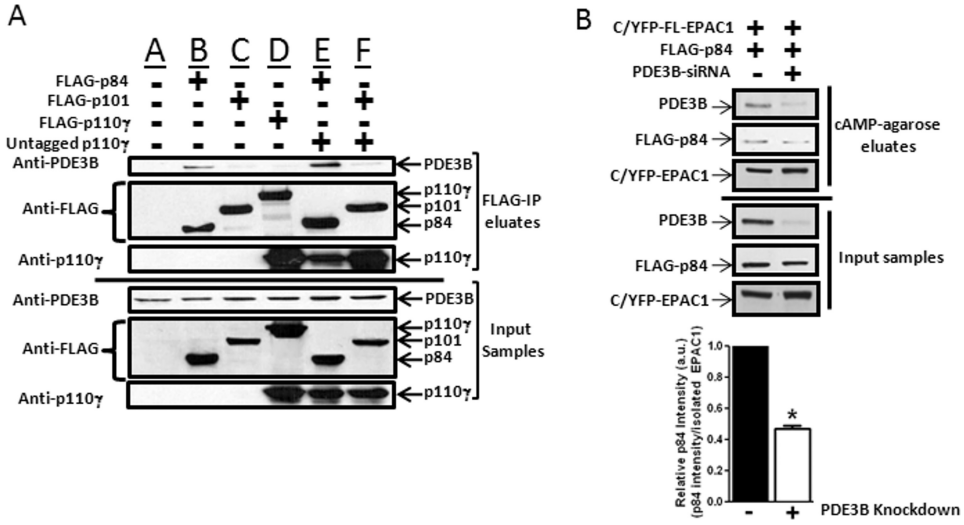

FIGURE 2. **PDE3B tethers EPAC1 and p84-p110γ.** *A*, separate 293T cell cultures transfected with plasmids individually encoding FLAG-tagged PI3Kγ subunits (FLAG-p84, FLAG-p101, or FLAG-p110γ) or with one of FLAG-p84 or FLAG-p101 and untagged p110γ were incubated with M2-agarose (4 °C, 16 h). Immune complexes were isolated, and PDE3B, FLAG, or p110γ was detected by immunoblot analysis. Immunoblots representative of data obtained in three experiments are shown. *B*, FLAG-p84 and C/YFP-EPAC1 were both expressed in 293T cells or 293T cells following PDE3B knockdown. PDE3B and p84 in EPAC1 isolates were detected by immunoblot analysis and quantified by densitometry. *, significant difference between p84 recovered from cells expressing reduced PDE3B and controls in three separate experiments.

ity may directly regulate EPAC1 binding of cellular cAMP. The EPAC-selective cAMP analog, 8-pCPT-2′-O-Me-cAMP, significantly increased GTP-loading of Rap-1 (126 ± 6% of control, $n = 3$) and R-Ras (197 ± 23%, $n = 3$) (Fig. 1*D*) in HEK293 cells, indicating that both of these G proteins can potentially transduce signals downstream from EPAC1 in cells.

PDE3B Binds p84 Selectively and Recruits PI3Kγ—Because global EPAC1 activation in cells can signal downstream through several effectors, including PI3K (11), and PDE3B had been reported to influence PI3Kγ-mediated effects in certain cell types (15, 21), we investigated whether the PDE3B-EPAC1 complex also integrated PI3Kγ. Consistent with this notion, we demonstrate that PDE3B binds one of the PI3Kγ regulatory subunits (p84) and that p84 binding is amplified in cells expressing the PI3Kγ catalytic domain (p110γ) (Fig. 2*A*). In contrast, the PDE3B-EPAC1 complex did not integrate the second PI3Kγ regulatory subunit or p110γ in the absence of p84 (Fig. 2*A*). Also consistent with p84 integration into the PDE3B-EPAC1 complex, PDE3B knockdown reduced levels of p84 recovered in EPAC1 pulldowns (Fig. 2*B*). Because PDE3B knockdown did not completely eliminate p84 recovery from EPAC1 isolates, further studies will be required to test the idea that EPAC1 and p84 also can interact independently of PDE3B. Regrettably, the p84 and p110γ antisera available to us did not allow these proteins to be directly immunoprecipitated from cell lysates.

PDE3B Interacts with EPAC1 and p84 Using Distinct Peptide Domains—We next set out to gain insight into the molecular determinants that underpin PDE3B-EPAC1 and PDE3B-p84 interactions using peptide array analysis, a powerful method for investigating the molecular nature of protein-protein interactions (3, 23). Using FLAG-PDE3B to interrogate peptide arrays encompassing the entire sequence of EPAC1, we identified two PDE3B-binding EPAC1 peptides, namely peptide 1 (Thr-218 to His-242) and peptide 2 (Glu-398 to Lys-422) (Fig. 3*A*). Although PDE3B binding was compromised by alanine substitution of several individual amino acid in peptide 1, alanine substitution of individual residues in peptide 2, including Asp-412, Gly-415, Phe-417, Asp-420, and Phe-421, completely ablated PDE3B binding, suggesting that PDE3B binding to peptide 2 was exquisitely sensitive to changes in its sequence (Fig. 3*A*). These data suggest that two PDE3B interaction sites exist in EPAC1: one located at the very start of the cAMP binding domain (peptide 1) and one within the Ras exchanger motif domain (peptide 2). Many protein-protein interactions involving PDEs and target proteins involve multiple binding sites, which facilitate the specificity of interaction (5).

Probing PDE3B peptide arrays with purified FLAG-EPAC1 identified a sequence at the extreme N-terminal region of PDE3B (Met-1 to Glu-25). Single alanine substitutions of several residues in this peptide including Arg-2, Arg-3, Arg-6, Lys-9, and Arg-12 ablated interactions (Fig. 3*B*). We also note that substitution of either Ala-8 or Ala-10 for Asp in this peptide reduced EPAC1 binding (Fig. 3*B*), a result consistent with the idea that placing a negatively charged residue in the midst of this positively charged region disrupts a key role in PDE3-EPAC1 interaction.

In addition to EPAC1-PDE3B binding, we also probed PDE3B peptide arrays with the three PI3Kγ subunits. In doing this, we observed that FLAG-p84 bound a peptide C-terminal to the second N-terminal hydrophobic region of PDE3B, which encompasses Pro-436 to Asn-460. Subsequent scanning array analyses showed that Ala substitution of any of Arg-439, Arg-440, Pro-449, and Ser-445 reduced p84 binding (Fig. 3*B*). Neither p101 nor p110γ bound peptides in PDE3B arrays (not shown).

Taken together, it is evident that probing a PDE3B array with either EPAC1 or p84 identified discrete interacting peptides where single amino acid substitutions could ablate binding. Because the PDE3B sequences involved in EPAC1 (Met-1 to

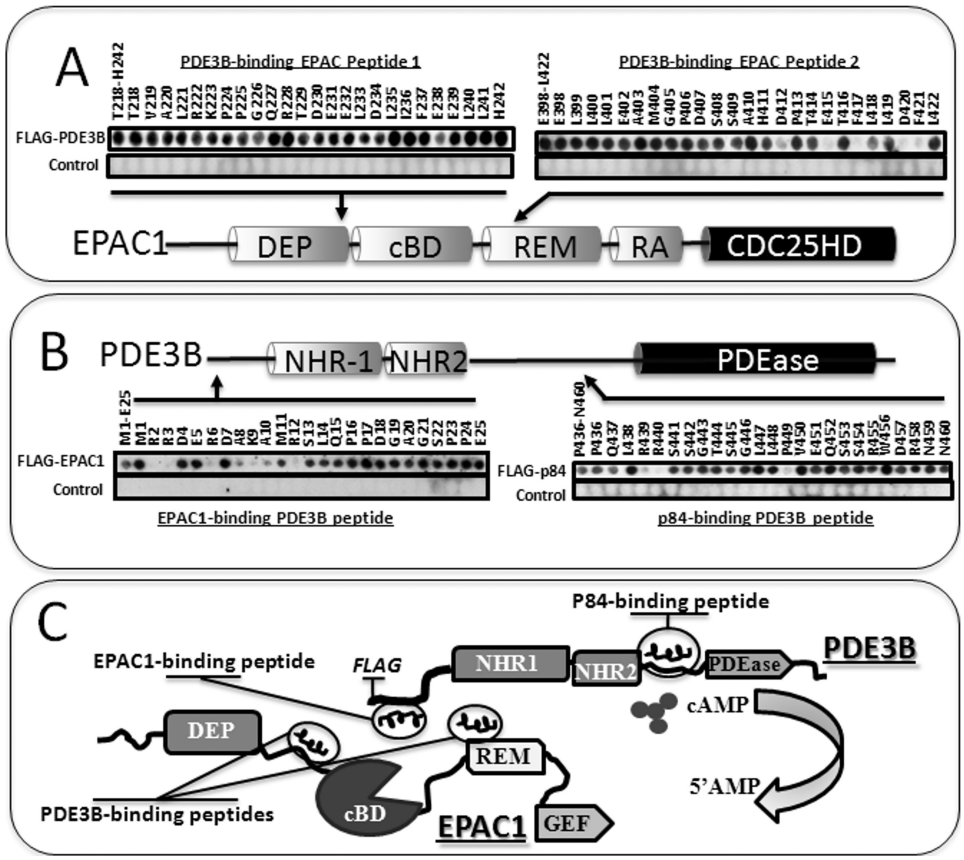

FIGURE 3. **Identification and analysis of PDE3B-EPAC or PDE3B-p84 interacting peptides.** *A*, individual membranes spotted with EPAC1 peptides (peptide 1, Thr-218 to His-242 or peptide 2, Glu-398 to Leu-422) in which each residue had been individually replaced with alanine were probed with a FLAG peptide solution (control) or a solution containing an N-terminally FLAG-tagged PDE3B (FLAG-PDE3B[AT]). FLAG binding was detected by immunoblotting (anti-FLAG, M2). *B*, membranes spotted with either an EPAC1-binding PDE3B peptides (Met-1 to Glu-25) or a p84-binding PDE3B peptide (Pro-436 to Asn-460) in which each residue had been individually replaced with alanine were probed with solutions containing either FLAG-EPAC1 or FLAG-p84, respectively. FLAG binding was detected by immunoblot analysis. A representative immunoblot from three similar experiments are shown. *C*, schematic representation of PDE3B-EPAC1 and PDE3B-p84 binding. In PDE3B, *NHR1* and *NHR2* are N-terminal hydrophobic membrane association regions 1 and 2, and *PDEase* depicts the catalytic domain. Shown in EPAC1 are the DEP (dishevelled, Egl-10, and pleckstrin) domain, cB (cyclic AMP binding) domain, the REM (Ras exchange motif), and GEF (guanine nucleotide exchange factor) catalytic domain.

Glu-25) or p84 (Pro-436 to Asn-460) binding did not overlap, these findings are consistent with the notion that PDE3B could simultaneously tether both EPAC1 and p84 in cells (Fig. 3*C*).

Human Arterial Endothelial Cells Contain a PDE3B/EPAC1/p84-PI3Kγ "signalosome" That Integrates Local EPAC1 and PI3Kγ Signals—We next assessed the role of PDE3B in tethering and regulating the activities of EPAC1 and p84-p110γ in HAECs. HAECs were chosen because they express PDE3B, EPAC1, and PI3Kγ endogenously (Fig. 4*A*), and previous work has shown that activation of EPAC1 or PI3Kγ can regulate their adhesion, migration, and permeability through ERK and/or PKB (1, 2, 13, 24, 25). Consistent with our studies in 293T cells, immunoprecipitation of endogenous HAEC PDE3B allowed co-isolation of endogenous EPAC1, p84, and p110γ, but not p101 (Fig. 4*B*). Also, knockdown of p84 but not p101 knockdown inhibited p110γ recovery in PDE3B immunoprecipitates by at least 50% ($n = 3$) (Fig. 4, *C* and *D*).

The PDE3 inhibitor (cilostamide, 1 μmol/liter) was used to test the hypothesis that cAMP hydrolysis by PDE3B was critical in allowing this PDE to control EPAC1-based activation of PI3Kγ in HAECs. Thus, cilostamide increased ERK (Fig. 5), and PKB (supplemental Fig. S1*A*) phosphorylation in HAECs and PI3Kγ inhibition with AS-604850 (3 μmol/liter) reversed these effects. Consistent with the effects of cilostamide, PDE3B knockdown markedly increased ERK (Fig. 5) and PKB (supplemental Fig. S1*A*) phosphorylation in HAECs and obviated any further increases with cilostamide. To evaluate whether direct EPAC1 activation could bypass PDE3B and directly promote PI3Kγ-mediated signaling, we used the EPAC-selective cAMP analog, 8-pCPT-2′-O-Me-cAMP. Although 8-pCPT-2′-O-Me-cAMP promoted the PI3Kγ inhibitor-sensitive phosphorylation of both ERK (Fig. 5) and PKB (supplemental Fig. S1*A*) in control HAECs, it did not increase ERK or PKB phosphorylation levels above those achieved upon PDE3B knockdown, indicating that PDE3B knockdown likely maximally activated PI3Kγ. Although HAEC p101 knockdown also increased ERK and PKB phosphorylation, the addition of cilostamide or 8-pCPT-2′-O-Me-cAMP could nonetheless still increase these effects in an AS-604850-sensitive manner in these cells. Overall, the observation that p84 but not p101 knockdown inhibited cilostamide-induced effects on ERK (Fig. 5) or PKB (supplemental Fig. S1*A*) phosphorylation indicates that cilostamide was likely acting selectively through the p84-regulated form of PI3Kγ in these cells.

Uncoupling EPAC1 from PDE3B Results in Increases in Local cAMP Signaling—Because we have shown that PDE3B and EPAC1 interact directly and that altering cellular levels of

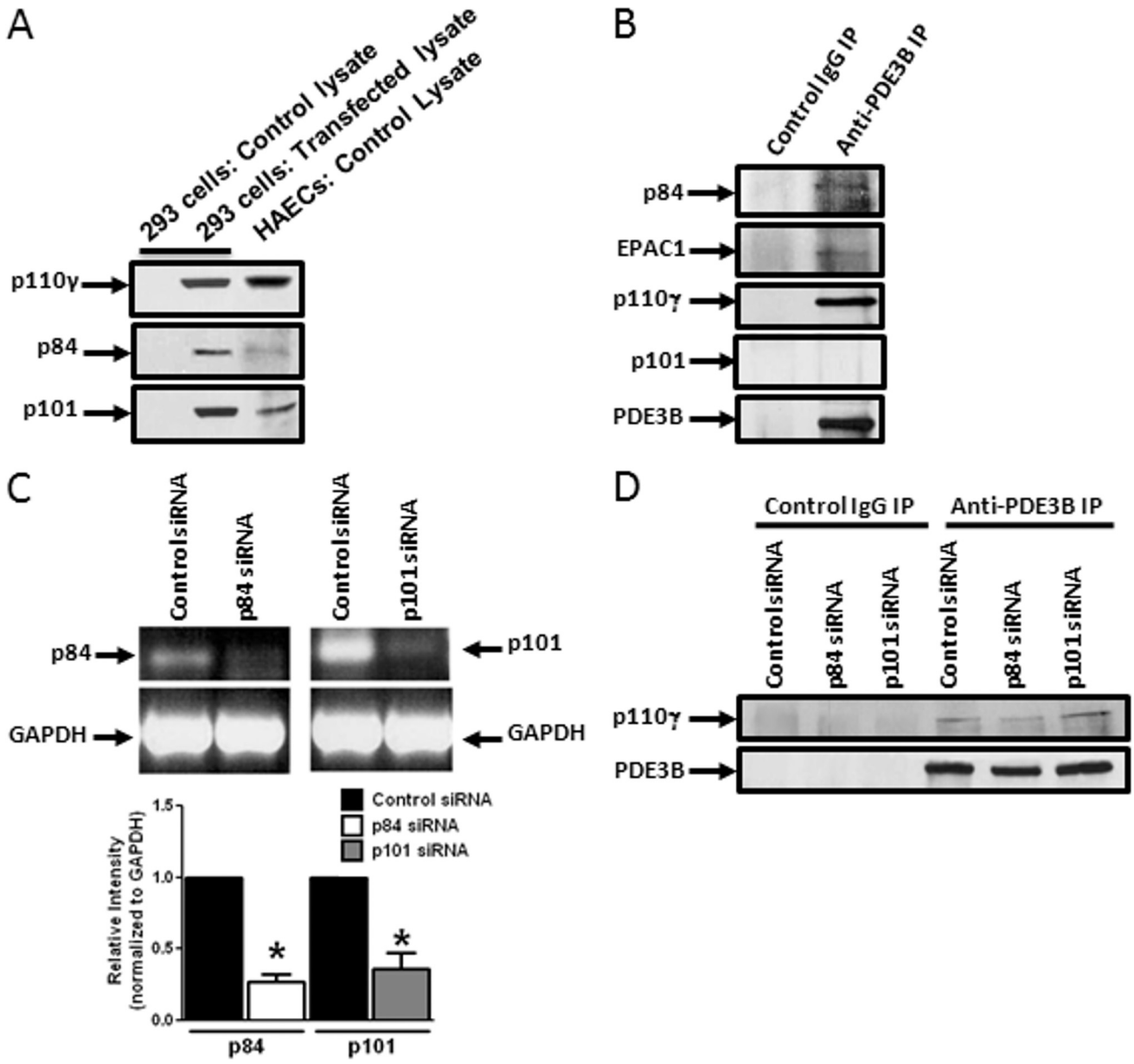

FIGURE 4. **A functional PDE3B/EPAC1/p84-p110γ complex is functional in HAECs.** *A*, immunoblot analysis indicates that HAECs express p110γ, p84, and p101 endogenously. *B*, proteins in control or anti-PDE3B immunoprecipitates (*IP*) derived from solubilized HAEC membrane fractions were immunoblotted for endogenous p84, EPAC1, p110γ, p101, and PDE3B. *C*, mRNA from HAEC transfected with either p84 or p101 siRNA was reverse transcribed and subjected to polymerase chain reaction using specific primers (see "Experimental Procedures"). Representative gels (*top panels*) and quantitation of results from three separate experiments (*bottom panel*) are shown. *, significant reductions in either p84 or p101 mRNA ($p < 0.05$). *D*, HAEC were transfected with either control, p84, or p101 siRNAs for 48 h, and membranes derived from lysates of these cells were immunoprecipitated with either normal mouse IgG or PDE3B antisera (4 °C, 16 h) and p110γ or PDE3B were detected by immunoblot analysis. p84 siRNA treatment significantly reduced levels of p110γ isolated in these experiments. Immunoblots representative of data obtained in four similar experiments are shown.

PDE3B impacted cAMP binding by an EPAC1-based cAMP sensor, we hypothesized that displacing EPAC1 from PDE3B should increase its ability to bind cAMP and therefore to activate PI3Kγ. To test this hypothesis, we designed a cell-permeable peptide capable of disrupting PDE3B-EPAC1 binding. Thus, because we observed that a Met-1 to Glu-25 PDE3B peptide variant containing only the first 13 residues and encompassing the critical cluster of basic residues effectively interacted with EPAC1 (supplemental Fig. S2*A*), an EPAC1-DP was created by linking Met-1 to Ser-13 to an N-terminal trans-activating transcriptional activator sequence (in bold type) via a short linker (*italics*) (**RKKRRQRRR**-*GG*-MRRDERDAKA-MRS). Similarly, a nondisplacing peptide (EPAC1-NDP) control was also generated in which the critical residues Arg-2, Arg-3, Arg-6, Lys-9, and Arg-12 were each substituted with Ala (**RKKRRQRRR**-*GG*-MAADEADAAAMAS).

As predicted, EPAC1-DP (10 μmol/liter), but not EPAC1-NDP (10 μmol/liter), inhibited direct EPAC1 binding to GST-PDE3B[1–90] *in vitro* and with PDE3B in cells (supplemental Fig. S2, *B* and *C*). Also, incubation with EPAC1-DP, but not EPAC1-NDP, promoted cAMP binding by an EPAC1-based cAMP sensor in response to forskolin (supplemental Fig. S2*D*), indicating that manipulation of EPAC1-PDE3B interactions results in altered local cAMP signaling in cells.

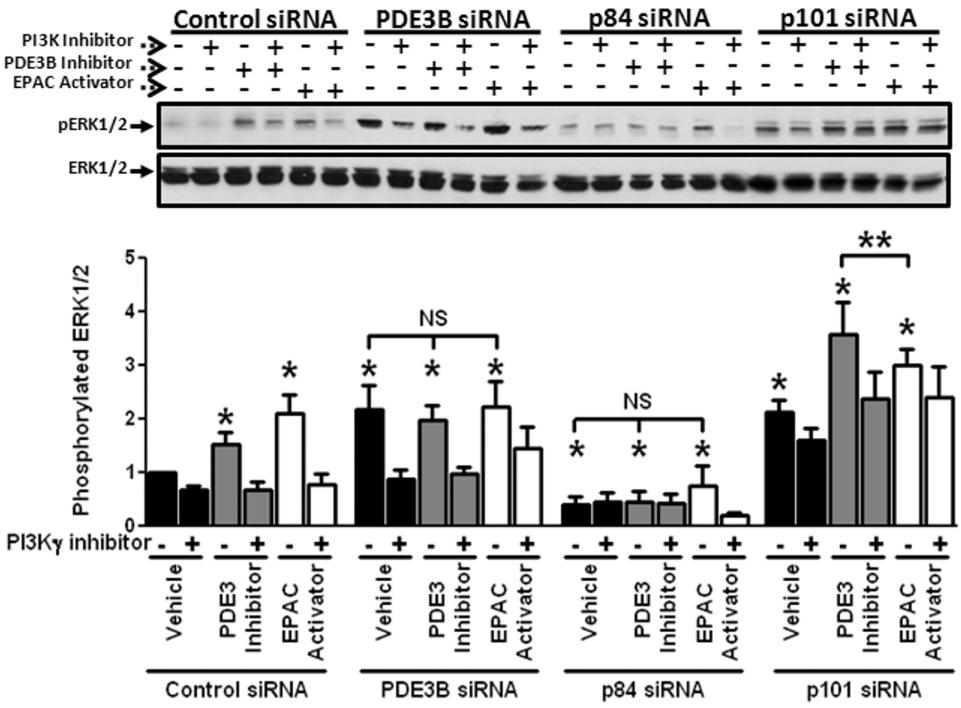

FIGURE 5. **PDE3B-dependent activation of ERK in HAECs.** Representative immunoblots of pERK1/2 accumulation in HAECs incubated with indicated agents (*top panel*) and quantitation of pERK1/2 (*bottom panel*) from five identical experiments (*bottom panel*) are shown. Individual HAEC cultures used were transfected with control, PDE3B, p84, or p101 siRNAs for 48 h, serum-starved overnight, and then incubated with a PDE3 inhibitor (cilostamide, 1 μmol/liter), an EPAC activator (8-pCPT-2′-O-Me-cAMP, 0.1 mmol/liter), a PI3Kγ inhibitor (AS-604850, 3 μmol/liter), or some of the agents in combination, for 5 min. ERK1/2 and pERK1/2 were detected by immunoblot analysis, and levels of these species were quantified by densitometry *, significant difference ($p < 0.05$) in ERK phosphorylation between control *versus* treatment or knockdown samples ($n = 5$). **, difference ($p < 0.05$) in ERK phosphorylation between control and cilostamide or 8-pCPT-2′-O-Me-cAMP in HAECs where p101 was knocked down ($n = 5$).

The hypothesis that PDE3B-based tethering of EPAC1 is critical for EPAC1-mediated activation of PI3Kγ downstream signaling in HAECs was similarly tested using these displacing peptides. Thus, EPAC1-DP (10 μmol/liter), but not EPAC1-NDP (10 μmol/liter) reduced recovery of endogenous EPAC1 and p110γ in PDE3B immunoprecipitates in HAECs (Fig. 6*A*). This provides compelling evidence that these endogenous proteins form a heterotrimeric complex in cells and that PDE3B-EPAC1 binding is important for PI3Kγ integration. Furthermore, EPAC1-DP, but not EPAC1-NDP, significantly promoted PI3Kγ-mediated phosphorylation of both ERK and PKB in HAECs (Fig. 6*B* and supplemental Fig. S1*B*) and obviated further increases upon either PDE3 inhibition with cilostamide or EPAC activation with 8-pCPT-2′-O-Me-cAMP. Again, the ERK and PKB phosphorylation caused by EPAC1-DP were reversed by AS-604850, demonstrating that this action was PI3Kγ-dependent (Fig. 6*B* and supplemental Fig. S1*B*).

Taken together, these data show that 1) a PDE3B-tethered EPAC1/p84-p110γ signalosome is present in HAECs; 2) this signalosome integrates EPAC1 and PI3Kγ signals; and 3) disruption of the complex by PDE3B knockdown or by displacing EPAC1 promotes cAMP binding to EPAC1 and EPAC1-dependent activation of PI3Kγ signaling. Moreover, because our studies were largely conducted without direct stimulation of adenylyl cyclase, our findings indicate that cAMP hydrolysis by PDE3B in HAECs may negatively regulate basal EPAC1-dependent actions on PI3Kγ and as such influence downstream ERK1/2- and PKB-dependent signals.

The PDE3B/EPAC1/PI3Kγ Signalosome Regulates HAEC Adhesion, Spreading, and Tubule Formation—Previous work in our laboratory showed that cilostamide and 8-pCPT-2′-O-Me-cAMP each stimulate HAEC adhesion to extracellular matrix-coated surfaces and that cilostamide inhibits HAEC migration (1, 2). Because endothelial cell adhesion, spreading, and migration are each important steps in angiogenesis (27), we next decided to test the hypothesis that PDE3, EPAC1, and PI3Kγ each regulated adhesion and spreading by actions coordinated through the PDE3B-based HAEC signalosome rather than generally throughout the cell and that these effects would impact the angiogenic potential of these cells.

Overall, our data are consistent with this hypothesis. Indeed, knockdown of individual components of the complex markedly altered HAEC adhesion (not shown) and cell spreading (Fig. 7*A*). Thus, whereas PDE3B knockdown promoted HAEC cell spreading by 20 $\pm$ 4% at 1 h, knockdown of EPAC1 or of p84 inhibited cell spreading by 52 $\pm$ 6 and 55 $\pm$ 8%, respectively, at this time point (Fig. 7*A*). Consistent with the idea that the PDE3B-based signalosome allowed compartmentation of PDE3B and EPAC1 in HAECs within structures involved in cellular adhesions and spreading, immunostaining of HAECs fixed during the act of adhering for PDE3B and EPAC1 showed that these proteins co-localized to punctuate, possibly membrane-associated, HAEC structures (Fig. 7*B*). This presents the exciting possibility that these structures represent dynamic cellular domains within which the PDE3B-based signalosome

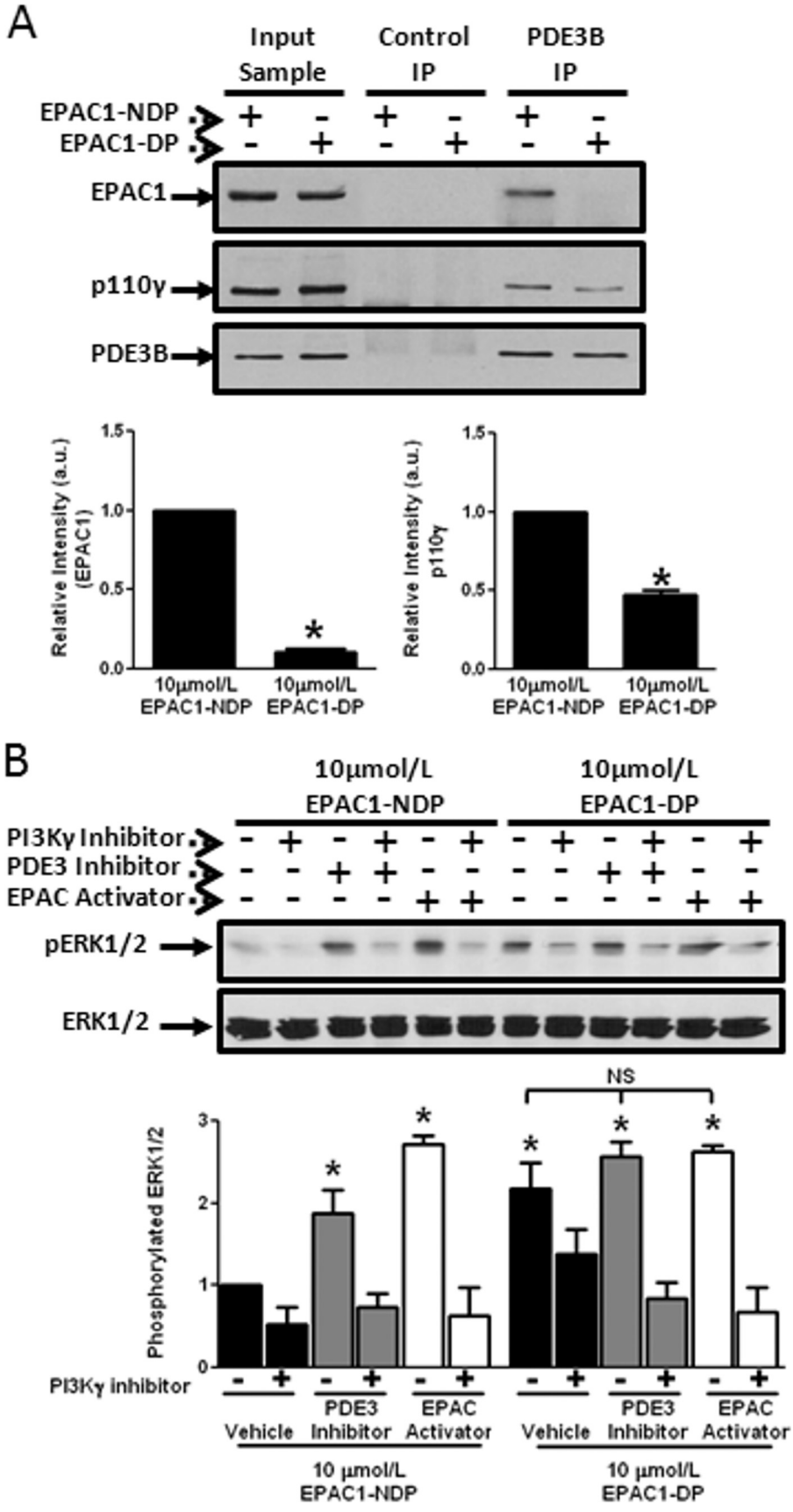
A
Input Sample
Control IP
PDE3B IP
EPAC1-NDP
EPAC1-DP
EPAC1
p110γ
PDE3B
Relative Intensity (a.u.) (EPAC1)
Relative Intensity (a.u.) p110γ
10μmol/L EPAC1-NDP
10μmol/L EPAC1-DP
B
10μmol/L EPAC1-NDP
10μmol/L EPAC1-DP
PI3Kγ Inhibitor
PDE3 Inhibitor
EPAC Activator
pERK1/2
ERK1/2
NS
Phosphorylated ERK1/2
PI3Kγ inhibitor
Vehicle
PDE3 Inhibitor
EPAC Activator
10 μmol/L EPAC1-NDP
10 μmol/L EPAC1-DP

identified here orchestrates the integration of EPAC1 and PI3Kγ signaling.

Consistent with the notion that these effects were due to signaling within the complex and that displacement of EPAC1 from PDE3B would allow EPAC1 to bind more cAMP and activate PI3Kγ, the addition of EPAC1-DP (10 μmol/liter), but not EPAC1-NDP (10 μmol/liter) significantly increased HAEC adhesion (Fig. 7*C*). As with their effects on signaling (Fig. 5), neither cilostamide nor EPAC1-DP promoted cell spreading in PDE3B knockdown cells or influenced cell spreading of HAECs in which EPAC1 or p84 had been knocked down. Importantly, each of these effects was fully antagonized by PI3Kγ inhibition. Indeed, basal cell spreading and the increased cell spreading of PDE3B knockdown cells were reduced by 32 ± 5% and 40 ± 5%, respectively, in the presence of AS-604850. PI3Kγ inhibition was without effect when EPAC1 or p84 were knocked down (not shown).

To directly test our prediction that signaling through the PDE3B-based signalosome promotes adhesion and spreading of HAECs and that these effects impact the angiogenic potential of these cells, we utilized an *in vitro* angiogenesis assay: the tubule formation assay. In this assay, adhesion, spreading, and migration of endothelial cells on Matrigel each promote the formation of branched primitive vessels (26). Although the addition of 8-pCPT-2′-O-Me-cAMP, cilostamide, or AS-604850 did not significantly alter the number of branch points or the overall pattern of the branched tubular structures formed by HAECs after 10 h on Matrigel, they did impact the relative "thickness" of branched structures formed (Fig. 7*D*). In contrast, cilostamide or 8-pCPT-2′-O-Me-cAMP significantly shortened the times at which endothelial cell "branch points," the earliest structures that form during tubule formation in this assay (26), were evident (Fig. 7*D*). Indeed, branch point formation was increased by 265 ± 4 or 193 ± 3% by 8-pCPT-2′-O-Me-cAMP or cilostamide at 1 h, respectively (Fig. 7, *D* and *F*). In contrast, AS-604850 increased the time at which branch points first appeared (Fig. 7, *D* and *F*). These results are consistent with the hypothesis that branch points formed faster in the presence of 8-pCPT-2′-O-Me-cAMP or cilostamide but slower in the presence of AS-604850 and that these differences were due to the effects of these agents on HAEC adhesion and spreading.

Consistent with this model and with the effects of cilostamide, PDE3B knockdown promoted early branch point formation and allowed formation of "thicker" tubules (Fig. 7*E*). Indeed, in the eight separate experiments in which this was measured, PDE3B knockdown increased the number of branch points at 1 h by 200 ± 5% (mean ± S.E.; Fig. 7, *E* and *F*) of control. Also, 8-pCPT-2′-O-Me-cAMP or cilostamide addition did not further increase the number of branch points formed in PDE3B knockdown cells (Fig. 7*F*). In contrast, but consistent with our model, knockdown of either EPAC1 or p84 significantly reduced the number of branch points present at 1 h and hindered the formation of stable structures (Fig. 7, *E* and *F*). Moreover, cilostamide or 8-pCPT-2′-O-Me-cAMP could not be used to rescue the poor responses observed in EPAC1 or p84 knockdown cells (Fig. 7*F*). Also, the addition of EPAC1-DP (10 μmol/liter) but not EPAC1-NDP (10 μmol/liter) markedly increased the numbers of branch points that were present in control HAECs but not PDE3B, EPAC1, or p84 knockdown cells (Fig. 7*G*). Consistent with the idea that only the p84-regulated form of PI3Kγ is subject to EPAC1-dependent regulation and involved in tubule formation through this complex, the decreased tubule formation in p101 knockdown cells was somewhat rescued by 8-pCPT-2′-O-Me-cAMP, cilostamide, or EPAC1-DP (Fig. 7, *F* and *G*).

In keeping with the known function of EPAC1, 8-pCPT-2′-O-Me-cAMP promoted accumulation of both GTP-bound Rap-1 (205 ± 12%, $n = 3$) and R-Ras (135% 9%, $n = 3$) in HAECs (supplemental Fig. S3*A*). However, only R-Ras knockdown significantly impacted tubule formation by those agents promoting tubule formation through the PDE3B-based signalosome (supplemental Fig. S3*B*). Indeed, although 8-pCPT-2′-O-Me-cAMP, cilostamide, or the EPAC1-DP each could promote tubule formation in Rap1A knockdown HAECs, these agents were ineffective when added to HAECs in which R-Ras had been knocked down (supplemental Fig. S3*B*). This result uncovers an intriguing facet indicating that the PDE3B-based signalosome may be specifically wired to function through R-Ras in these cells. Thus, PDE3B may sequester EPAC1/p84-PI3Kγ to a spatially defined domain that serves to channel signals through a specific effector system.

DISCUSSION

The results of the present study identify a novel signaling complex formed from PDE3B/EPAC1/p84 that integrates EPAC1- and PI3Kγ-encoded signals in human arterial endothelial cells. This signalosome may provide a cellular context within which EPAC and PI3Kγ are integrated and may represent a novel therapeutic target for the design of agents able to control specific endothelial cell functions, including their angiogenic potential.

Components of the PDE3B-tethered Complex—It is increasingly evident that protein-protein interactions aid in spatially organizing cellular signal transduction and regulation of cellular function (2, 5–8). Here we have identified and characterized a novel signaling complex (signalosome) that contains PDE3B, EPAC1, and, selectively, the p84-regulated form of PI3Kγ. Our analyses suggest that PDE3B and EPAC1 interact directly with each other in this complex, without the need for any accessory proteins or lipids, and that endogenous species form an endog-

FIGURE 6. **Disruption of endogenous PDE3B-EPAC1 binding in HAECs alters PI3Kγ signaling.** *A*, HAECs were incubated with EPAC1-NDP or EPAC1-DP (10 μmol/liter) for 4 h. Membrane fractions were isolated and immunoprecipitated (*IP*) with control IgG or anti-PDE3B IgG (4 °C, 16 h). Isolated immune complexes were immunoblotted for EPAC1, p110γ, and PDE3B. Representative immunoblots (*top panels*) and quantification values obtained from three separate experiments (*bottom panels*) are shown. *, significant difference ($p < 0.05$) in EPAC1 and p110γ recovered between groups. *B*, following incubation of HAECs with EPAC1-DP or EPAC1-NDP (10 μmol/liter, 4 h), the cells were incubated with either a PDE3 inhibitor (cilostamide, 1 μmol/liter) or an EPAC1 activator (8-pCPT-2′-O-Me-cAMP, 0.1 mmol/liter) in the absence or presence of a PI3Kγ inhibition (AS-604850, 3 μmol/liter). Accumulation of pERK1/2 in HAECs following these treatments was investigated by immunoblot analyses. Representative immunoblots (*top panels*) and quantification of results obtained in three similar experiments (*bottom panels*) are shown. *, significant difference ($p < 0.05$) in ERK1/2 phosphorylation between control and treated groups; *NS*, lack of difference.

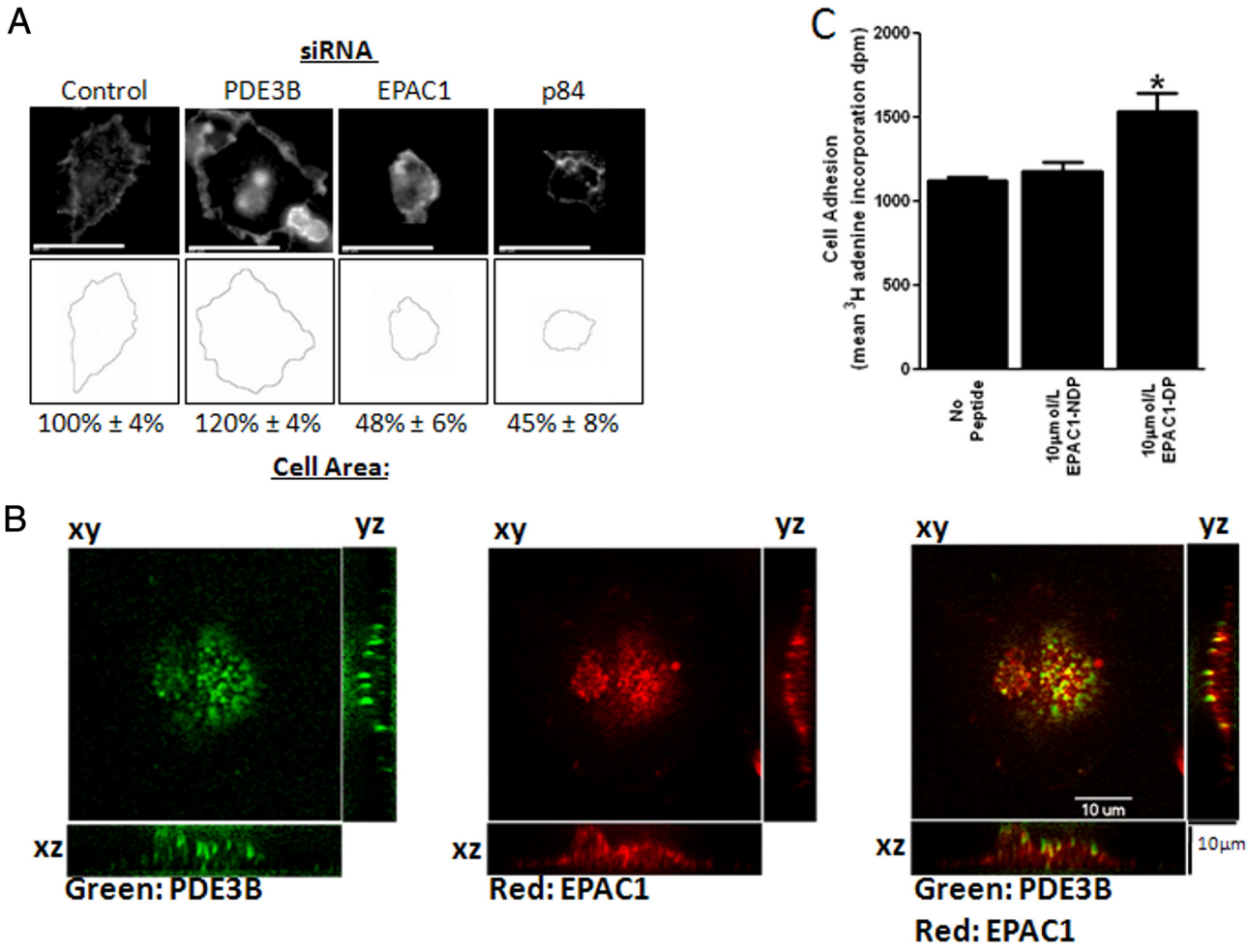
A
siRNA
Control
PDE3B
EPAC1
p84
100% ± 4%
120% ± 4%
48% ± 6%
45% ± 8%
Cell Area:
C
Cell Adhesion
(mean ^{3}H adenine incorporation dpm)
2000
1500
1000
500
0
*
No Peptide
10µmol/L EPAC1-NDP
10µmol/L EPAC1-DP
B
xy
yz
xz
Green: PDE3B
Red: EPAC1
10 um
10µm
Green: PDE3B
Red: EPAC1
D
Additions
Control
EPAC Activator
PDE3 inhibitor
PI3Kγ inhibitor
1 hour
10 hours
E
siRNA
Control
PDE3B
EPAC1
p84
1 hour
10 hour
F
# of Branch Points
40
30
20
10
0
Vehicle
EPAC Activator
PDE3 Inhibitor
PI3Kγ Inhibitor
Control siRNA
PDE3B siRNA
EPAC1 siRNA
p84 siRNA
p101 siRNA
G
# of Branch Points
EPAC1-NDP
EPAC-DP
EPAC1-DP
NS
Control siRNA
PDE3B siRNA
EPAC1 siRNA
p84 siRNA
p101 siRNA

enous intracellular complex in human endothelial cells. Consistent with previous studies on murine heart (15, 21), we show here that PDE3B interacts with the p84 regulatory subunit of PI3Kγ and go on to expand on this, proposing that PDE3B likely acts to simultaneously tether both EPAC1 and p84 to form a functional complex in endothelial cells that controls tubule formation and has implications for angiogenesis.

Regulation of Signaling through the PDE3B-based Signalosome—Converging signaling is a common theme, and usually the efficiency of signal integration is enhanced when enzymes are grouped within signaling complexes. In our studies, we have uncovered two instances where a proposed PDE3B/EPAC1/p84–110γ signaling complex promotes cAMP and PI3Kγ signaling. First, using a FRET-based approach, we show that cAMP binding, by EPAC1, was markedly altered by either varying PDE3B cellular levels or by directly displacing EPAC1 from its PDE3B tether using a PDE3B-based displacing peptide (EPAC1-DP). Together, these data establish PDE3B as a "sink" for degrading the pool of cAMP that activates EPAC1 in cells and thus serves to maintain EPAC1 in a suboptimally activated state up to the point when cAMP generation is elevated to such an extent that it overwhelms the degrading capacity of complexed PDE3B. Because displacing EPAC1 from its PDE3B tether directly increased its cAMP binding, we conclude that the proximity of PDE3B and EPAC1 within this complex is critical to the ability of PDE3B to control EPAC1 activation by cAMP. Lending further support to this proposal, cAMP binding to this same EPAC1-based sensor was unaffected when PDE4B or PDE4D was individually knocked down in an earlier report by some of us (27). Because PDE4B and PDE4D together account for ~65% of total cAMP-PDE activity in the cells used in these studies, we propose that our data indicate that EPAC1 binding to PDE3B likely contributes to this selectively.

Second, our studies demonstrated that inhibition of PDE3, activation of EPAC1, and displacement of EPAC1 from PDE3B each promoted PI3Kγ activation and subsequent phosphorylation of ERK and PKB. These findings support the idea that PDE3B-mediated control of EPAC1 activity allows the indirect cAMP-dependent regulation of PI3Kγ. In addition, selective knockdown of PDE3B resulted in increased basal ERK and PKB phosphorylation. Although this result was initially surprising to us, we concluded that the basal cAMP hydrolyzing activity of PDE3B maintains a low level of local cAMP, thus maintaining EPAC1 in an inactive state. This regulation of signaling has been documented before in the cAMP field with the discovery of A-kinase anchoring proteins, which bind to PKA and target this kinase to distinct subcellular locals but can maintain this kinase in a low activity setting by sequestering PDE4 isoforms (28). Here, we propose that PDE3B tethers EPAC1, maintaining a low activity that protects it from inappropriate fluctuations in basal cAMP levels until a significant directed increase in cAMP generation occurs that overwhelms the capacity of sequestered PDE3B.

Cardiac myocytes represent the cardiovascular cell type in which PI3Kγ has been most extensively studied (29), and hearts from p110γ-null mice have elevated cAMP and display an exaggerated contractile response. Although early reports proposed that p110γ tethered an activated form of PDE3B (21) and that the absence of this interaction in p110γ-null mice caused their cardiac phenotype, our findings further refine this model, suggesting that PDE3B may indirectly sequester p110γ through p84, as proposed earlier (15). Indeed, because levels of each p84 and p101 are profoundly reduced in cells devoid of p110γ (17), we predict that p110γ-null mice may express reduced p84 levels and that this secondary effect could contribute to the aberrant PDE3B-regulated cAMP and the contractile phenotype.

Regulation of HAEC Functions through the PDE3B-tethered Complex—Angiogenesis represents a complex process in which endothelial cell function is critical. Initial pro-angiogenic signals result in the adhesion, spreading, migration, and proliferation of endothelial cells, resulting in the formation of tubular structures and the eventual maturation of these structures into stable blood vessels (30). Both the cAMP and polyphosphatidylinositol signaling systems impact each of these endothelial cell functions and as such likely regulate angiogenesis. In these studies, we observed that inhibition of PDE3B and direct activation of EPAC1 each promoted HAEC tubule formation and that these effects were inhibited by PI3Kγ inhibition. In addition, using RNAi-based approaches, we show here that the actions of cilostamide or 8-pCPT-2′-O-Me-cAMP are coordinated through actions involving EPAC1, R-Ras, and selectively the p84-regulated, but not the p101-regulated, form of PI3Kγ.

Intriguingly, we found that R-Ras but not Rap1 was the most likely G protein transducing information between EPAC1 and PI3Kγ in HAECs. Indeed, although EPAC1 can activate both R-Ras and Rap1 in HAECs, only R-Ras knockdown antagonized the response of HAECs to 8-pCPT-2′-O-Me-cAMP, cilostamide, or EPAC1-DP. How our findings can be related to previ-

FIGURE 7. **Integration of EPAC1 and p84-p110γ promotes HAEC tubule formation by stimulating cell adhesion and spreading.** *A*, individual HAEC cultures were transfected with control, PDE3B, EPAC1, or p84 siRNAs for 48 h. Transfected HAECs were trypsinized and allowed to adhere to Matrigel for 15 min. Representative images from five equivalent experiments of fixed cells stained for actin after 15 min on Matrigel are shown. Mean cell areas (# of pixels occupied) for cells transfected with the various constructs were calculated using ImageJ and are expressed as percentages of the control cell areas. *B*, samples of control HAECs allowed to adhere to fibronectin-coated surfaces for 15 min were fixed and immunostained for PDE3B (*green*) and EPAC1 (*red*). Similar staining was observed in several individual cells sampled in three separate experiments. *C*, HAECs were incubated with no peptide, 10 μmol/liter EPAC1-NDP, or 10 μmol/liter EPAC1-DP and allowed to adhere to fibronectin-coated surfaces. The values are the means ± S.E. of four determinations. *, significant difference ($p < 0.05$) between cells incubated with EPAC1-DP and those incubated with either EPAC1-NDP or without peptide. *D*, extent of tubule formation at 1 and 10 h, and impact of control (Me_2SO, 0.1% v/v), EPAC activator (0.1 mmol/liter, 8-pCPT-2′-O-Me-cAMP), PDE3 inhibitor (1 μmol/liter, cilostamide), and PI3Kγ inhibitor (3 μmol/liter, AS-604850). Representative images from eight equivalent experiments are shown. *E*, extent of tubule formation and impact of control, PDE3B, EPAC1, and p84 siRNA at 1 and 10 h post-plating on Matrigel. Representative images from eight equivalent experiments are shown. *F*, images from *D* and *E* were skeletonized using Image J, and the numbers of branch points formed at 1 h were counted manually in a blinded manner. HAEC were transfected with indicated siRNA and allowed to form tubes in the presence of vehicle (Me_2SO 1% v/v), EPAC activator (0.1 mmol/liter, 8-pCPT-2′-O-Me-cAMP), PDE3 inhibitor (0.1 μmol/liter, cilostamide), or PI3Kγ inhibitor (3 μmol/liter, AS-604850). *, significant difference ($p < 0.05$) between control and treatment or siRNA knockdown. #, significant difference ($p < 0.05$) between treatment and control of the same group of siRNA-treated cells. *G*, individual HAEC cultures were transfected with control, PDE3B, EPAC1, p84, or p101 siRNAs as described above, and the impact of EPAC1-NDP (10 μmol/liter) or EPAC1-DP (10 μmol/liter) on tubule formation was measured. *, significant difference ($p < 0.05$). The values are the means ± S.E. of eight experiments.

ous work in which R-Ras allowed EPAC2 to regulate phospholipase D(9) or in which Ras was described as an "indispensable co-regulator" of p84-p110γ activation (20) will require further study.

Although PI3K signaling regulates blood vessel formation and vascular repair (25, 31), a limited amount of information is available currently regarding involvement of specific PI3K isoforms in these processes. Recently PI3Kα was reported to regulate angiogenic sprouting vascular remodeling but not initial stages of vascular development (25). Here, we show that EPAC1-mediated activation of p84-p110γ promotes several initial events in this process including adhesion and spreading and that these events correlate strongly with tubule formation. Also, recent studies indicating an essential role for EPAC1 and PI3Kγ in optimal integrin-dependent homing of endothelial progenitor cells to sites of vascularization (31, 32) may represent another area where signaling similar to that described here also regulates vascular events of importance in wound repair and angiogenesis.

In conclusion, we provide compelling evidence that PDE3B-tethered EPAC1 is regulated by PDE3B-mediated hydrolysis of cAMP, that activation of the "pool" of EPAC1 in this novel signalosome promotes p84-p110γ-mediated phosphorylation of ERK and PKB, and that these effects regulate several cellular events in endothelial cells of importance in cardiovascular health and disease.

REFERENCES

1. Netherton, S. J., and Maurice, D. H. (2005) *Mol. Pharmacol.* **67,** 263–272
2. Netherton, S. J., Sutton, J. A., Wilson, L. S., Carter, R. L., and Maurice, D. H. (2007) *Circ. Res.* **101,** 768–776
3. Rampersad, S. N., Ovens, J. D., Huston, E., Umana, M. B., Wilson, L. S., Netherton, S. J., Lynch, M. J., Baillie, G. S., Houslay, M. D., and Maurice, D. H. (2010) *J. Biol. Chem.* **285,** 33614–33622
4. Dodge-Kafka, K. L., Soughayer, J., Pare, G. C., Carlisle Michel, J. J., Langeberg, L. K., Kapiloff, M. S., and Scott, J. D. (2005) *Nature.* **437,** 574–578
5. Houslay, M. D. (2010) *Trends Biochem. Sci.* **35,** 91–100
6. Raymond, D. R., Wilson, L. S., Carter, R. L., and Maurice, D. H. (2007) *Cell Signal.* **19,** 2507–2518
7. Houslay, M. D., Baillie, G. S., and Maurice, D. H. (2007) *Circ. Res.* **100,** 950–966
8. Pawson, C. T., and Scott, J. D. (2010) *Nat. Struct. Mol. Biol.* **17,** 653–658
9. López De Jesús, M., Stope, M. B., Oude Weernink, P. A., Mahlke, Y., Börgermann, C., Ananaba, V. N., Rimmbach, C., Rosskopf, D., Michel, M. C., Jakobs, K. H., and Schmidt, M. (2006) *J. Biol. Chem.* **281,** 21837–21847
10. Schmidt, M., Evellin, S., Weernink, P. A., von Dorp, F., Rehmann, H., Lomasney, J. W., and Jakobs, K. H. (2001) *Nat. Cell Biol.* **3,** 1020–1024
11. Gloerich, M., and Bos, J. L. (2010) *Annu. Rev. Pharmacol. Toxicol.* **50,** 355–375
12. Johnson, C., Marriott, S. J., and Levy, L. S. (2007) *Oncogene.* **26,** 7049–7057
13. Funamoto, S., Meili, R., Lee, S., Parry, L., and Firtel, R. A. (2002) *Cell.* **109,** 611–623
14. Crackower, M. A., Oudit, G. Y., Kozieradzki, I., Sarao, R., Sun, H., Sasaki, T., Hirsch, E., Suzuki, A., Shioi, T., Irie-Sasaki, J., Sah, R., Cheng. H. Y., Rybin, V. O., Lembo, G., Fratta, L., Oliveira-dos-Santos, A. J., Benovic, J. L., Kahn, C. R., Izumo, S., Steinberg, S. F., Wymann, M. P., Backx, P. H., and Penninger, J. M. (2002) *Cell* **110,** 737–749
15. Voigt, P., Dorner, M. B., and Schaefer, M. (2006) *J. Biol. Chem.* **281,** 9977–9986
16. Stephens, L. R., Eguinoa, A., Erdjument-Bromage, H., Lui, M., Cooke, F., Coadwell, J., Smrcka, A. S., Thelen, M., Cadwallader, K., Tempst, P., and Hawkins, P. T. (1997) *Cell.* **89,** 105–114
17. Suire, S., Coadwell, J., Ferguson, G. J., Davidson, K., Hawkins, P., and Stephens, L. (2005) *Curr. Biol.* **15,** 566–570
18. Stoyanov, B., Volinia, S., Hanck, T., Rubio, I., Loubtchenkov, M., Malek, D., Stoyanova, S., Vanhaesebroeck, B., Dhand, R., and Nürnberg, B. (1995) *Science* **269,** 690–693
19. Suire, S., Hawkins, P., and Stephens, L. (2002) *Curr. Biol.* **12,** 1068–1075
20. Kurig, B., Shymanets, A., Bohnacker, T., Prajwal Brock, C., Ahmadian, M. R., Schaefer, M., Gohla, A., Harteneck, C., Wymann, M. P., Jeanclos, E., and Nürnberg, B. (2009) *Proc. Natl. Acad. Sci. U.S.A.* **106,** 20312–20317
21. Patrucco, E., Notte, A., Barberis, L., Selvetella, G., Maffei, A., Brancaccio, M., Marengo, S., Russo, G., Azzolino, O., Rybalkin, S. D., Silengo, L., Altruda, F., Wetzker, R., Wymann, M. P., Lembo, G., and Hirsch, E. (2004) *Cell* **118,** 375–387
22. Bjørgo, E., Solheim, S. A., Abrahamsen, H., Baillie, G. S., Brown, K. M., Berge, T., Okkenhaug, K., Houslay, M. D., and Taskén, K. (2010) *Mol. Cell. Biol.* **30,** 1660–1672
23. Bolger, G. B., Baillie, G. S., Li, X., Lynch, M. J., Herzyk, P., Mohamed, A., Mitchell, L. H., McCahill, A., Hundsrucker, C., Klussmann, E., Adams, D. R., and Houslay, M. D. (2006) *Biochem. J.* **398,** 23–36
24. Marone, R., Cmiljanovic, V., Giese, B., and Wymann, M. P. (2008) *Biochim. Biophys. Acta.* **1784,** 159–185
25. Graupera, M., Guillermet-Guibert, J., Foukas, L. C., Phng, L. K., Cain, R. J., Salpekar, A., Pearce, W., Meek, S., Millan, J., Cutillas, P. R., Smith, A. J., Ridley, A. J., Ruhrberg, C., Gerhardt, H., and Vanhaesebroeck, B. (2008) *Nature* **453,** 662–666
26. Arnaoutova, I., George, J., Kleinman, H. K., and Benton, G. (2009) *Angiogenesis.* **12,** 267–274
27. Terrin, A., Di Benedetto, G., Pertegato, V., Cheung, Y. F., Baillie, G., Lynch, M. J., Elvassore, N., Prinz, A., Herberg, F. W., Houslay, M. D., and Zaccolo, M. (2006) *J. Cell Biol.* **175,** 441–451
28. McCahill, A., McSorley, T., Huston, E., Hill, E. V., Lynch, M. J., Gall, I., Keryer, G., Lygren, B., Tasken, K., van Heeke, G., and Houslay, M. D. (2005) *Cell Signal.* **17,** 1158–1173
29. Damilano, F., Perino, A., and Hirsch, E. (2010) *Ann. N.Y. Acad. Sci.* **1188,** 39–45
30. Yancopoulos, G. D., Davis, S., Gale, N. W., Rudge, J. S., Wiegand, S. J., and Holash, J. (2000) *Nature* **407,** 242–248
31. Chavakis, E., Carmona, G., Urbich, C., Göttig, S., Henschler, R., Penninger, J. M., Zeiher, A. M., Chavakis, T., and Dimmeler, S. (2008) *Circ. Res.* **102,** 942–949
32. Carmona, G., Chavakis, E., Koehl, U., Zeiher, A. M., and Dimmeler, S. (2008) *Blood.* **111,** 2640–2646